IEEE Photonics Journal
An IEEE Photonics Society Publication

Open Access

Quaternion Approach to the Measurement of the Local Birefringence Distribution in Optical Fibers

Volume 7, Number 4, August 2015

Lanlan Liu
Chongqing Wu
Chao Shang
Zhengyong Li
Jian Wang

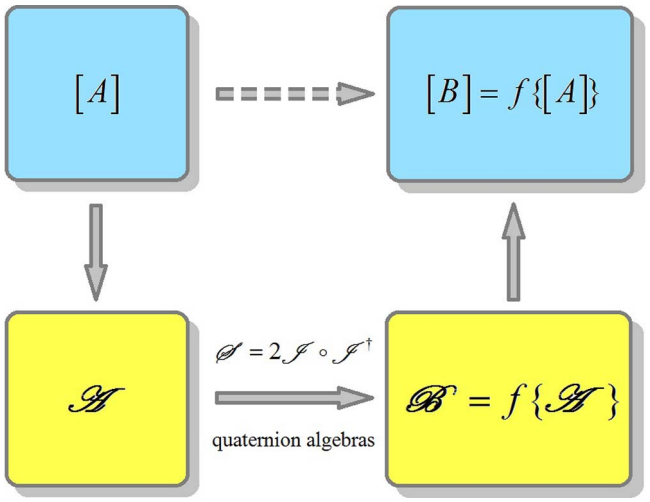

DOI: 10.1109/JPHOT.2015.2445096
1943-0655

Quaternion Approach to the Measurement of the Local Birefringence Distribution in Optical Fibers

Lanlan Liu,[1] Chongqing Wu,[1] Chao Shang,[2] Zhengyong Li,[1] and Jian Wang[1]

[1]Institute of Optical Information, School of Science, Key Laboratory of Education, Ministry on Luminescence and Optical Information Technology, Beijing Jiaotong University, Beijing 100044, China
[2]State Key Laboratory of Information Photonics and Optical Communications, School of Electronic Engineering, Beijing University of Posts and Telecommunications, Beijing 100876, China

DOI: 10.1109/JPHOT.2015.2445096

Manuscript received February 25, 2015; revised June 2, 2015; accepted June 9, 2015. Date of publication June 15, 2015; date of current version July 23, 2015. This work was supported in part by the National Natural Science Foundation of China under Grant 61275075 and in part by Beijing Natural Science Foundation under Grant 4132035 and Grant 4144080. Corresponding author: C. Wu (e-mail: cqwu@bjtu.edu.cn).

Abstract: A method to structure the Jones quaternion utilizing Pauli matrices is proposed, improving the quaternion theory of polarization optics. It is proved that the Stokes quaternion is the double product of the Jones quaternion and its Hermitian transpose and that the rotation axis of the output three-adjacent-point Stokes quaternions is a mapping from the rotation axis of the three-adjacent-reflection-point Stokes quaternions in the optical fiber and that the rotation angle among the output three adjacent points is the doubleness of the rotation angle among the three adjacent reflection points in the optical fiber. The three-point quaternion method to measure birefringence distribution is proposed and implemented, the experimental result shows that the average birefringence is 0.263/m in the fiber under test, and the corresponding average beat length is 26 m. We also demonstrated the paraxial approximate quaternion Baker–Campbell–Hausdorff formula of exponential quaternions multiplying for cascaded optical components; then, a quaternion interpolation method to estimate the error of birefringence measurement is proposed, and the relative error calculated was less than 5%. The previously cited works indicate that the quaternion algorithm is very effective in the research of the polarization in optical fibers.

Index Terms: Birefringence quaternion, Jones quaternion, polarization optics, fiber optics.

1. Introduction

It is well known that, because of non-circular cross-section, mechanical stress, and bending in optical fibers, single-mode optical fibers become birefringent mediums [1]. This birefringence will influence the performances of optical fiber rings in the fiber optic gyroscopes and fiber optic current sensors seriously [2], [3] and act as a major factor for the polarization mode dispersion [4], [5]. Furthermore, birefringence can cause crosstalk, polarization instability and other problems in the polarization multiplexing optical fiber communication systems. Therefore, the accurate measurement of the local birefringence distribution is a significant work.

The relationship between birefringence and the bending radius of the optical fiber was reported by R. Ulrich *et al.* under no axial stress situation [6], and the average birefringence due

to bending was analyzed and measured. Block *et al.* analyzed the birefringence caused by optical fiber cladding bending utilizing vector wave equation [7]. Rogers proposed polarization-sensitive optical time domain reflectometry (P-OTDR) [8], and the birefringence distribution in the optical fiber was calculated by the different polarization states of the Rayleigh scattered light. Since P-OTDR was proposed, there are many articles on in-depth theoretical and experimental researches for P-OTDR [9]–[13]. A P-OTDR system based on piezoelectric polarization controller (PPC-assisted P-OTDR) was reported, it realized the measurement of distributed birefringence in the optical fiber [14]. All of schemes above are calculating the polarization properties by Mueller matrix, in which the optical fiber is divided into many short segments, which are described by Mueller matrices, and the entire optical fiber Mueller matrix is the cascade of all the short segment Mueller matrices, but in the calculation, a coordinate inversion matrix must be inserted in the middle of two adjacent Mueller matrices due to the reflection of light. A series of recursive calculation must be done to obtain Mueller matrix of every segment, which makes the operation particularly complex.

Quaternion was proposed in 1843 by W. R. Hamilton, who was a famous Irish mathematician [15]; this discovery is one of the most significant events of 19th century algebra. Quaternion multiplication has the synthesized characteristics of numerical multiplication, multiplication of scalar and vector, dot and cross multiplications of vector, which ensure that the product of two quaternions is still a quaternion. The inverse of quaternion, the quaternion exponentiation function, and the quaternion transcendental function can also be defined, they constitute a complete system of quaternion algebra. In polarization optics, the Stokes parameters used for describing the state of polarization (SOP), containing a scalar s_0 and a three-dimensional vector $[s_1, s_2, s_3]^{\mathrm{T}}$, which makes it associated with quaternion description. In 2004, M. Karlsson and M. Petersson used quaternion to analyze the polarization mode dispersion and polarization-dependent gain in optical fibers [16]. In 2013, a literature proposed the quaternion can be used to analyze the SOP [17]. Furthermore, the quaternion methods to describe the SOP of light and the polarized optical components and systems were theoretically derived based on Poincaré sphere and quaternion representations [18].

In this paper, quaternion is utilized as a mathematical tool to study the problems of the local birefringence in the optical fiber. First, in Section 2, we improved the theory of quaternion polarization optics, the corresponding quaternion had been derived to describe Jones vector, Jones matrix and Stokes vector, defined as the Jones quaternion, Mueller quaternion, and Stokes quaternion. It is proved that Stokes quaternion is double product of Jones quaternion and its Hermitian transpose by the theoretical calculation. Second, in Section 3, we proposed a three-point quaternion method to measure birefringence distribution in optical fibers, and in Section 4, completed the distributed measurement of the local birefringence quaternion's vectorial parts, which included magnitude and direction. In order to estimate the error of this measurement method, a quaternion interpolation algorithm was proposed according to paraxial approximate quaternion Baker–Campbell–Hausdorff formula in Section 5.

2. Quaternion Polarization Optics

In this article, the quaternion method is equivalent to one pair of transformation. A 2×2 matrix can be decomposed as follows:

$$[A]_{2\times 2} = a_0\sigma_0 + \boldsymbol{A}\cdot\vec{\sigma} \tag{1}$$

where $\sigma_0 = \begin{bmatrix} 1 & \\ & 1 \end{bmatrix}$, and $\vec{\sigma} = \left(\begin{bmatrix} 1 & \\ & -1 \end{bmatrix}, \begin{bmatrix} & 1 \\ 1 & \end{bmatrix}, \begin{bmatrix} & -i \\ i & \end{bmatrix}\right)^{\mathrm{T}}$. It is a matrix vector composed by three Pauli matrices. We can construct a quaternion (represented by Edward Script ITC font) using the parameters a_0 and $\boldsymbol{A} = [a_x, a_y, a_z]^{\mathrm{T}}$ in (1). It can be written as

$$\mathscr{A} = a_0 + i\boldsymbol{A} = a_0 + i(a_x\hat{\boldsymbol{i}} + a_y\hat{\boldsymbol{j}} + a_z\hat{\boldsymbol{k}}) \tag{2}$$

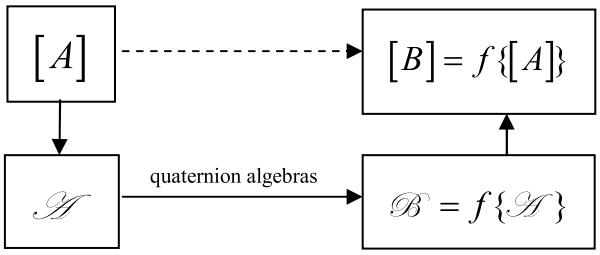

Fig. 1. Basic idea of quaternion polarization optics.

where $i = \sqrt{-1}$, $\hat{\boldsymbol{i}}, \hat{\boldsymbol{j}}, \hat{\boldsymbol{k}}$ are the unit vectors of three coordinates x, y, z in Cartesian coordinate system, respectively. Then, such a matrix will correspond with a quaternion

$$[A] \leftrightarrow \mathscr{A}. \tag{3}$$

The decomposition of (1) is unique; thus, the constructed quaternion is unique, but they are not equal. It can be proven that the constructed quaternion not only satisfy the rule of quaternion operations, but also has a significant rule that the operation results is equivalent for all analytical matrices and theirs corresponding quaternions. Therefore, there is an equivalence theorem: if an operation to make $[B] = f\{[A]\}$, certainly $\mathscr{B} = f\{\mathscr{A}\}$, and *vice versa*.

Accordingly, the vectors or matrix can be rewritten as quaternion for calculations, and then the results can be transformed back to the vectors or matrices. This method will change the complex matrix operations into simple quaternion algebras. The basic idea of quaternion polarization optics is shown in Fig. 1.

The concepts and algebraic algorithms of quaternion can be found in the relevant literatures. In this paragraph, the correspondences between quaternion and some of the basic concepts in polarization optics will be discussed as follows.

2.1. Quaternion Description for Jones Vector

According to the wave theory of light, the polarized light field can be described by Jones vector $\boldsymbol{J} = [\dot{E}_x,\ \dot{E}_y]^{\mathrm{T}}$ [19]. In order to find a corresponding quaternion, the Jones vector can be written as an equivalent matrix $\begin{bmatrix} \dot{E}_x & 0 \\ \dot{E}_y & 0 \end{bmatrix}$ by adding zero elements. Therefore, the Jones vector corresponding quaternion (Jones quaternion) is expressed as

$$\mathscr{J} = \frac{\dot{E}_x}{2} + i\frac{\dot{E}_x}{2}\hat{\boldsymbol{i}} + i\frac{\dot{E}_y}{2}\hat{\boldsymbol{j}} + \frac{\dot{E}_y}{2}\hat{\boldsymbol{k}}. \tag{4}$$

Because of $|\mathscr{J}| = 0$, the inverse of $\mathscr{J}$ does not exist, and it is impossible to do division operations. Obviously, its Hermitian transpose $\boldsymbol{J}^{\dagger} = \begin{bmatrix} \dot{E}_x^* & \dot{E}_y^* \\ 0 & 0 \end{bmatrix}$, and the corresponding quaternion is expressed as

$$\mathscr{J}^{\dagger} = \frac{\dot{E}_x^*}{2} + i\frac{\dot{E}_x^*}{2}\hat{\boldsymbol{i}} + i\frac{\dot{E}_y^*}{2}\hat{\boldsymbol{j}} - \frac{\dot{E}_y^*}{2}\hat{\boldsymbol{k}}. \tag{5}$$

2.2. Quaternion Description for Stokes Vector

According to the rule of quaternion multiplication (we use $\circ$ to denote multiplying quaternion), the product of Jones quaternion $\mathscr{J}$ and its Hermitian transpose $\mathscr{J}^{\dagger}$ is easy to be calculated, and the double product can be described as

$$2\mathscr{J} \circ \mathscr{J}^{\dagger} = s_0 + is_1\hat{\boldsymbol{i}} + is_2\hat{\boldsymbol{j}} + is_3\hat{\boldsymbol{k}} \tag{6}$$

where [20]

$$s_0 = \dot{E}_x\dot{E}_x^* + \dot{E}_y\dot{E}_y^*, \quad s_1 = \dot{E}_x\dot{E}_x^* - \dot{E}_y\dot{E}_y^*, \quad s_2 = \dot{E}_x\dot{E}_y^* + \dot{E}_x^*\dot{E}_y, \quad s_3 = i\left(\dot{E}_x\dot{E}_y^* - \dot{E}_x^*\dot{E}_y\right). \quad (7)$$

Therefore, the Stokes quaternion can be defined as

$$\mathscr{S} = s_0 + i\boldsymbol{s} = s_0 + is_1\hat{\boldsymbol{i}} + is_2\hat{\boldsymbol{j}} + is_3\hat{\boldsymbol{k}} \quad (8)$$

where $\boldsymbol{s} = [s_1, s_2, s_3]^{\mathrm{T}}$, thus the relationship between Stokes quaternion and Jones quaternion can be expressed as

$$\mathscr{S} = 2\mathscr{J} \circ \mathscr{J}^{\dagger}. \quad (9)$$

2.3. Quaternion Description for Optical Components

When a beam of polarized light propagates through an optical element, there are three basic effects: birefringence, namely the polarization dependent phase shift; polarization dependent loss or gain (PDL\PDG); and polarization coupling, in other words, the energy coupling between orthogonal SOPs. Normally, the first two effects are considered more generally, and the third effect will usually occur in the optical fibers.

2.3.1. Birefringent Component (Wave Plate)

It can be assumed that the x axis of selected coordinate system is consistent with the polarization principal axis direction $\hat{\boldsymbol{n}}_0$ of the birefringent component, namely $\hat{\boldsymbol{i}} = \hat{\boldsymbol{n}}_0$; then, its Jones matrix can be written as

$$\boldsymbol{U} = \begin{bmatrix} e^{i\varphi_x} & \\ & e^{i\varphi_y} \end{bmatrix} = e^{i\bar{\varphi}}\begin{bmatrix} e^{-i\Delta\varphi/2} & \\ & e^{i\Delta\varphi/2} \end{bmatrix} = e^{i\bar{\varphi}}\left\{a_0\begin{bmatrix} 1 & \\ & 1 \end{bmatrix} + a_x\begin{bmatrix} 1 & \\ & -1 \end{bmatrix} + a_y\begin{bmatrix} 0 & 1 \\ 1 & 0 \end{bmatrix} + a_z\begin{bmatrix} & -i \\ i & \end{bmatrix}\right\} \quad (10)$$

where $\bar{\varphi} = (\varphi_x + \varphi_y)/2$, $\Delta\varphi = \varphi_y - \varphi_x$. It is easy to calculate that

$$a_0 = \cos(\Delta\varphi/2), \quad a_x = -i\sin(\Delta\varphi/2), \quad a_y = a_z = 0. \quad (11)$$

Using (2), the corresponding quaternion $\mathscr{M}_{\mathrm{B}}$ can be expressed as

$$\mathscr{M}_{\mathrm{B}} = e^{i\bar{\varphi}}(a_0 + ia_x\hat{\boldsymbol{i}}) = e^{i\bar{\varphi}}\left\{\cos(\Delta\varphi/2) + \hat{\boldsymbol{i}}\sin(\Delta\varphi/2)\right\} = \exp[i\bar{\varphi} + \hat{\boldsymbol{i}}\Delta\varphi/\boldsymbol{2}]. \quad (12)$$

Taking into account $\hat{\boldsymbol{i}} = \hat{\boldsymbol{n}}_0$

$$\mathscr{M}_{\mathrm{B}} = \exp[i\bar{\varphi} + \hat{\boldsymbol{n}}_0\Delta\varphi/\boldsymbol{2}]. \quad (13)$$

In order to distinguish between the Jones vector corresponding quaternion and the Jones matrix corresponding quaternion, we call them respectively Jones quaternion and Mueller quaternion. Please note that Mueller quaternion is not the Mueller matrix [21] corresponding quaternion.

2.3.2. Polarization Dependent Loss Component

It can be assumed that the x axis of selected coordinate system is consistent with the polarization principal axis direction $\hat{\boldsymbol{n}}_0$ of the polarization dependent loss component, namely $\hat{\boldsymbol{i}} = \hat{\boldsymbol{n}}_0$, then its transmission matrix can be written as

$$\boldsymbol{U} = \begin{bmatrix} e^{-\alpha_x/2} & \\ & e^{-\alpha_y/2} \end{bmatrix} = e^{-\frac{\bar{\alpha}}{2}}\begin{bmatrix} e^{-\Delta\alpha/4} & \\ & e^{\Delta\alpha/4} \end{bmatrix} = e^{-\frac{\bar{\alpha}}{2}}\left\{\cosh\frac{\Delta\alpha}{4}\begin{bmatrix} 1 & \\ & 1 \end{bmatrix} - \sinh\frac{\Delta\alpha}{4}\begin{bmatrix} 1 & \\ & -1 \end{bmatrix}\right\} \quad (14)$$

where $\bar{\alpha} = (\alpha_x + \alpha_y)/2$, $\Delta\alpha = \alpha_y - \alpha_x$, α_x, and α_y are the optical power attenuation coefficients. After a simple calculation and taking into account $\hat{\boldsymbol{i}} = \hat{\boldsymbol{n}}_0$, the corresponding Mueller quaternion

$\mathscr{M}_{\mathrm{PDL}}$ can be expressed as

$$\mathscr{M}_{\mathrm{PDL}} = e^{-\bar{\alpha}/2}\left\{\cosh\frac{\Delta\alpha}{4} - i\sinh\frac{\Delta\alpha}{4}\hat{\boldsymbol{i}}\right\} = \exp[-\bar{\alpha}/2 + \hat{\boldsymbol{n}}_0(-i\Delta\alpha/4)]. \tag{15}$$

Synthesized considering (13) and (15), if it can be assumed that the two principal axis directions of birefringent polarization and the polarization dependent loss in an optical component are consistent, the corresponding quaternion $\mathscr{M}$ of common optical components can be expressed as

$$\mathscr{M} = \exp[-\bar{\alpha}/2 + i\bar{\varphi} + \hat{\boldsymbol{n}}_0(\Delta\varphi/2 - i\Delta\alpha/4)]. \tag{16}$$

Equation (16) can describe all the optical propagation characteristics of optical components, such as the average attenuation, the average phase shift, polarization-dependent loss (or PDG-polarization dependent gain) and polarization-dependent phase shift. In addition, it is more concise compared with 4 $\times$ 4 Mueller matrix.

2.4. Quaternion Description for Polarized Lights Propagating Through Optical Components

According to the theories above, we can use quaternions to fully describe the polarization properties of optical systems.

Jones quaternion methods: The relationship between the quaternion of the input polarized light and the quaternion of the output polarized light can be described as

$$\mathscr{J}_{\mathrm{out}} = \mathscr{M} \circ \mathscr{J}_{\mathrm{in}} \tag{17}$$

where $\mathscr{M}$ is the quaternion of optical components.

Stokes quaternion methods: According to (9) and (17), the output Stokes quaternion can be calculated as

$$\mathscr{S}_{\mathrm{out}} = 2(\mathscr{M}\boldsymbol{J}_{\mathrm{in}}) \circ (\mathscr{M}\boldsymbol{J}_{\mathrm{in}})^{\dagger} = \mathscr{M}(2\mathscr{J}_{\mathrm{in}} \circ \mathscr{J}_{\mathrm{in}}^{\dagger})\mathscr{M}^{\dagger} = \mathscr{M}(\mathscr{S}_{\mathrm{in}})\mathscr{M}^{\dagger} \tag{18}$$

where $\mathscr{S}_{\mathrm{in}}$ and $\mathscr{S}_{\mathrm{out}}$ are the input and output Stokes quaternion, respectively. Therefore the calculation formula of the Stokes quaternion can be expressed as

$$\mathscr{S}_{\mathrm{out}} = \mathscr{M}(\mathscr{S}_{\mathrm{in}})\mathscr{M}^{\dagger}. \tag{19}$$

Substituting (16) into (19), then (20) can be obtained as

$$\mathscr{S}_{\mathrm{out}} = e^{-\bar{\alpha}+\hat{\boldsymbol{n}}_0(\Delta\varphi/2 - i\Delta\alpha/4)} \circ (\mathscr{S}_{\mathrm{in}}) \circ e^{-\hat{\boldsymbol{n}}_0(\Delta\varphi/2 - i\Delta\alpha/4)}. \tag{20}$$

When considering only the vector parts of $\mathscr{S}_{\mathrm{out}}$ and $\mathscr{S}_{\mathrm{in}}$, and $\mathscr{S}_{\mathrm{in}} = s_{\mathrm{in0}} + \boldsymbol{S}_{\mathrm{in}}$, $\mathscr{S}_{\mathrm{out}} = s_{\mathrm{out0}} + \boldsymbol{S}_{\mathrm{out}}$, in addition, if it can be assumed that only the effect of birefringence exists in the optical component can be obtained as

$$s_{\mathrm{out0}} = e^{-\alpha}s_{\mathrm{in0}}, \quad \boldsymbol{S}_{\mathrm{out}} = \exp(\hat{\boldsymbol{n}}_0\Delta\varphi/2) \circ \boldsymbol{S}_{\mathrm{in}} \circ \exp(-\hat{\boldsymbol{n}}_0\Delta\varphi/2). \tag{21}$$

Equation (21) indicates that $\boldsymbol{S}_{\mathrm{out}}$ is the rotation result from $\boldsymbol{S}_{\mathrm{in}}$ with the angle $\Delta\varphi$ around the axis $\hat{\boldsymbol{n}}_0$ on Poincaré sphere.

3. Principle of the Birefringence Quaternion Distribution Measurement in Optical Fibers

3.1. Quaternion Description for the Backscatter Light in a Short Segment of Optical Fiber

For measurement of the local birefringence quaternion, firstly, we consider the backscatter light quaternion in a short segment of optical fiber. If $\mathscr{S}_1$ is the Stokes quaternion at the

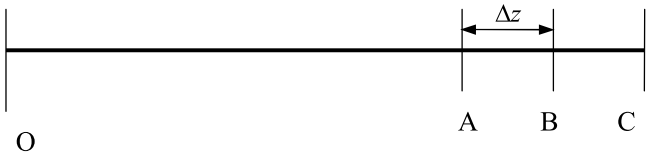

Fig. 2. Schematic diagram of the Stokes quaternion calculation at adjacent positions.

reflection point, $\mathscr{S}_{\text{in}}$ and $\mathscr{S}_{\text{out}}$ are the Stokes quaternions of the incidence and reflected back to the input port of this segment, respectively, the birefringence quaternion (Mueller quaternion) of this segment can be described as $\mathscr{M} = \exp[i\bar{\varphi} + \hat{\boldsymbol{n}}_0 \Delta\varphi/\mathbf{2}]$. We assume that the length of this segment is short enough that its polarization rotation axis $\hat{\boldsymbol{n}}_0$ remains unchanged, and $\Delta\varphi$ is proportional to this segment length Δz, namely $\Delta\varphi = \Delta\beta\Delta z$, where $\Delta\beta$ is the propagation constant difference of the two orthogonal polarization directions.

According to (20), neglecting the attenuation, $\mathscr{S}_1$ can be written as follows:

$$\mathscr{S}_1 = e^{\hat{\boldsymbol{n}}_0 \Delta\varphi/\mathbf{2}} \circ \mathscr{S}_{\text{in}} \circ e^{-\hat{\boldsymbol{n}}_0 \Delta\varphi/\mathbf{2}}. \tag{22}$$

Assuming that the SOP of the reflection light remains unchanged at the reflection point, and there is no energy coupling or exchange of the x and y polarized components, the SOP of the reflected back light at the input port is a further rotation from the SOP of the reflection point around the polarization rotation axis of this segment. Therefore, the relationship between the output Stokes quaternion and the input Stokes quaternion can be expressed as

$$\mathscr{S}_{\text{out}} = e^{\hat{\boldsymbol{n}}_0 \Delta\varphi/\mathbf{2}} \circ \mathscr{S}_1 \circ e^{-\hat{\boldsymbol{n}}_0 \Delta\varphi/\mathbf{2}}. \tag{23}$$

Substituting (22) into (23), because both polarization rotations have the same axis, therefore according to the exponential multiplication formula of the base number quaternions, equation (24) can be obtained as

$$\mathscr{S}_{\text{out}} = e^{\hat{\boldsymbol{n}}_0 \Delta\varphi} \circ \mathscr{S}_{\text{in}} \circ e^{-\hat{\boldsymbol{n}}_0 \Delta\varphi}. \tag{24}$$

It is more concise compared with the expression of Mueller matrix.

3.2. Basic Theory of the Three Point Quaternion Method

In this paragraph, we will discuss the relationship between the output SOP change at the start point of the entire fiber and the SOP change of each short segment. Assuming that there are two adjacent short segments in a long fiber, it is shown in Fig. 2. Generally for commercial single mode fiber, the beat length is about 5 m to 50 m, and the change of beat length accompanied by the change of polarization axis, the lengths of AB and BC should be shorter than 1 m.

Provided that $\mathscr{S}(A)$, $\mathscr{S}(B)$, and $\mathscr{S}(C)$ are the Stokes quaternions of the position A, B, and C, according to the theoretical derivations above, the Stokes quaternion $\mathscr{S}_A(B)$ which describes the light propagating from position A to B and reflecting back to position A can be expressed as

$$\mathscr{S}_A(B) = e^{[-2\alpha\Delta z + \hat{\boldsymbol{n}}_0 \Delta\beta\Delta z]} \circ \mathscr{S}(A) \circ e^{[-\hat{\boldsymbol{n}}_0 \Delta\beta\Delta z]}. \tag{25}$$

Similarly, the Stokes quaternion $\mathscr{S}_A(C)$, which describes the light propagating from position A to C and reflecting back to position A, can be expressed as

$$\mathscr{S}_A(C) = e^{2[-2\alpha\Delta z + \hat{\boldsymbol{n}}_0 \Delta\beta\Delta z]} \circ \mathscr{S}(A) \circ e^{2[-\hat{\boldsymbol{n}}_0 \Delta\beta\Delta z]}. \tag{26}$$

The three different SOP described by three quaternions $\mathscr{S}(A)$, $\mathscr{S}_A(B)$, and $\mathscr{S}_A(C)$ should propagate through the same route to the start point O of the fiber, although these processes are very complicated, we still divide the whole fiber into many segments named $L_1, L_2, \ldots, L_N$, whose

Mueller quaternion is $\mathscr{M}_i$. In ordinary fiber, the polarization dependent loss is negligible, and the $\mathscr{M}_i = \exp[-\bar{\alpha}/2 + i\bar{\varphi}_i + \hat{\boldsymbol{n}}_{0i}(\Delta\varphi_i/2)]$; thus

$$\mathscr{S}_{\text{out}}(A)=e^{[-\alpha L_A+i\phi]}\left[e^{\hat{\boldsymbol{n}}_{01}\Delta\varphi_1/2}\circ e^{\hat{\boldsymbol{n}}_{02}\Delta\varphi_2/2}\circ\cdots\circ e^{\hat{\boldsymbol{n}}_{0N}\Delta\varphi_N/2}\circ\mathscr{S}(A)\circ e^{-\hat{\boldsymbol{n}}_{0N}\Delta\varphi_N/2}\circ\cdots\circ e^{-\hat{\boldsymbol{n}}_{02}\Delta\varphi_2/2}\circ e^{-\hat{\boldsymbol{n}}_{01}\Delta\varphi_1/2}\right] \tag{27}$$

where $\phi = \sum\bar{\varphi}_i$, $L_A = \sum L_i$. Because the product of exponential function quaternions is still an exponential function quaternion, we let

$$e^{\hat{\boldsymbol{m}}\varphi/2} = \left[e^{\hat{\boldsymbol{n}}_{01}\Delta\varphi_1/2}\circ e^{\hat{\boldsymbol{n}}_{02}\Delta\varphi_2/2}\circ\cdots\circ e^{\hat{\boldsymbol{n}}_{0N}\Delta\varphi_N/2}\right]. \tag{28}$$

It is proved that

$$\left[e^{-\hat{\boldsymbol{n}}_{0N}\Delta\varphi_N/2}\circ\cdots\circ e^{-\hat{\boldsymbol{n}}_{02}\Delta\varphi_2/2}\circ e^{-\hat{\boldsymbol{n}}_{01}\Delta\varphi_1/2}\right] = \left[e^{\hat{\boldsymbol{n}}_{01}\Delta\varphi_1/2}\circ e^{\hat{\boldsymbol{n}}_{02}\Delta\varphi_2/2}\circ\cdots\circ e^{\hat{\boldsymbol{n}}_{0N}\Delta\varphi_N/2}\right]^{-1} = \left(e^{-\hat{\boldsymbol{m}}\varphi/2}\right). \tag{29}$$

Thus, the three output Stokes quaternions can be written as follows:

$$\mathscr{S}_{\text{out}}(A) = e^{[-2\alpha L_A+\hat{\boldsymbol{m}}\varphi]/2}\circ\mathscr{S}(A)\circ e^{[-\hat{\boldsymbol{m}}\varphi]/2} \tag{30}$$

$$\mathscr{S}_{\text{out}}(B) = e^{[-2\alpha L_A+\hat{\boldsymbol{m}}\varphi]/2}\circ\mathscr{S}_A(B)\circ e^{[-\hat{\boldsymbol{m}}\varphi]/2} \tag{31}$$

$$\mathscr{S}_{\text{out}}(C) = e^{[-2\alpha L_A+\hat{\boldsymbol{m}}\varphi]/2}\circ\mathscr{S}_A(C)\circ e^{[-\hat{\boldsymbol{m}}\varphi]/2}. \tag{32}$$

Therefore, according to (20), $\mathscr{S}_{\text{out}}(A)$, $\mathscr{S}_{\text{out}}(B)$, and $\mathscr{S}_{\text{out}}(C)$ can be seen as the results of the coordinate rotation from $\mathscr{S}(A)$, $\mathscr{S}_A(B)$, and $\mathscr{S}_A(C)$ on Poincaré sphere. As a result, the corresponding relationships among $\mathscr{S}_{\text{out}}(A)$, $\mathscr{S}_{\text{out}}(B)$, and $\mathscr{S}_{\text{out}}(C)$ are consistent with the corresponding relationships among $\mathscr{S}(A)$, $\mathscr{S}_A(B)$, and $\mathscr{S}_A(C)$. From (30), we obtained $\mathscr{S}(A) = e^{\alpha L_A}[e^{[-\hat{\boldsymbol{m}}\varphi]/2}\circ\mathscr{S}_{\text{out}}(A)\circ e^{[\hat{\boldsymbol{m}}\varphi]/2}]$, and substituting into (31) and (32) and considering (25) and (26), can get

$$\mathscr{S}_{\text{out}}(B) = e^{-2\alpha\Delta z}\left\{e^{[\hat{\boldsymbol{m}}\varphi]/2}\circ e^{[\hat{\boldsymbol{n}}_0\Delta\beta\Delta z]}\circ e^{[-\hat{\boldsymbol{m}}\varphi]/2}\circ\mathscr{S}_{\text{out}}(A)\circ e^{[\hat{\boldsymbol{m}}\varphi]/2}\circ e^{[-\hat{\boldsymbol{n}}_0\Delta\beta\Delta z]}\circ e^{[-\hat{\boldsymbol{m}}\varphi]/2}\right\} \tag{33}$$

$$\mathscr{S}_{\text{out}}(C) = e^{-4\alpha\Delta z}\left\{e^{[\hat{\boldsymbol{m}}\varphi]/2}\circ e^{2[\hat{\boldsymbol{n}}_0\Delta\beta\Delta z]}\circ e^{[-\hat{\boldsymbol{m}}\varphi]/2}\circ\mathscr{S}_{\text{out}}(A)\circ e^{[\hat{\boldsymbol{m}}\varphi]/2}\circ e^{2[-\hat{\boldsymbol{n}}_0\Delta\beta\Delta z]}\circ e^{[-\hat{\boldsymbol{m}}\varphi]/2}\right\}. \tag{34}$$

Let

$$e^{\hat{\boldsymbol{n}}_{\text{map}}\theta} = e^{[\hat{\boldsymbol{m}}\varphi]/2}\circ e^{[\hat{\boldsymbol{n}}_0\Delta\beta\Delta z]}\circ e^{[-\hat{\boldsymbol{m}}\varphi]/2}. \tag{35}$$

Thus

$$\mathscr{S}_{\text{out}}(B) = e^{-2\alpha\Delta z}e^{\hat{\boldsymbol{n}}_{\text{map}}\theta}\mathscr{S}_{\text{out}}(A)e^{-\hat{\boldsymbol{n}}_{\text{map}}\theta}. \tag{36}$$

In (34), due to

$$\begin{aligned} e^{[\hat{\boldsymbol{m}}\varphi]/2}\circ e^{2[\hat{\boldsymbol{n}}_0\Delta\beta\Delta z]}\circ e^{[-\hat{\boldsymbol{m}}\varphi]/2} &= e^{[\hat{\boldsymbol{m}}\varphi]/2}\circ e^{[\hat{\boldsymbol{n}}_0\Delta\beta\Delta z]}\circ e^{[\hat{\boldsymbol{n}}_0\Delta\beta\Delta z]}\circ e^{[-\hat{\boldsymbol{m}}\varphi]/2} \\ &= e^{[\hat{\boldsymbol{m}}\varphi]/2}\circ e^{[\hat{\boldsymbol{n}}_0\Delta\beta\Delta z]}\circ e^{[-\hat{\boldsymbol{m}}\varphi]/2}\circ e^{[\hat{\boldsymbol{m}}\varphi]/2}\circ e^{[\hat{\boldsymbol{n}}_0\Delta\beta\Delta z]}\circ e^{[-\hat{\boldsymbol{m}}\varphi]/2} \\ &= e^{\hat{\boldsymbol{n}}_{\text{map}}\theta}\circ e^{\hat{\boldsymbol{n}}_{\text{map}}\theta} = e^{2\hat{\boldsymbol{n}}_{\text{map}}\theta} \end{aligned} \tag{37}$$

we get

$$\mathscr{S}_{\text{out}}(C) = e^{-4\alpha\Delta z}e^{2\hat{\boldsymbol{n}}_{\text{map}}\theta}\mathscr{S}_{\text{out}}(A)e^{-2\hat{\boldsymbol{n}}_{\text{map}}\theta}. \tag{38}$$

Comparing (36) and (38) with (25) and (26), we can obtain the following conclusion: the rotation angle between $\mathscr{S}_{\text{out}}(A)$, $\mathscr{S}_{\text{out}}(B)$, and $\mathscr{S}_{\text{out}}(C)$ is the same as the rotation angle between

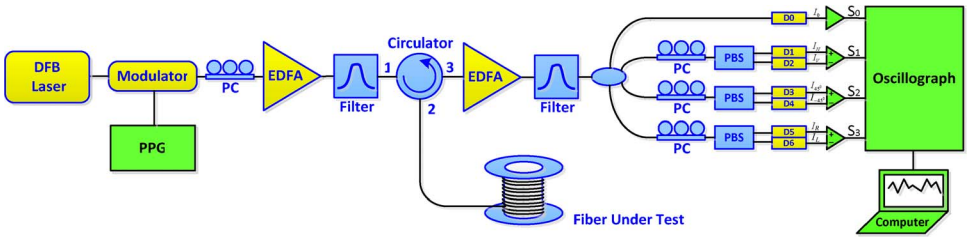

Fig. 3. Schematic of the local birefringence quaternion distribution measurement system.

$\mathscr{A}(A)$, $\mathscr{A}_A(B)$, and $\mathscr{A}_A(C)$; the rotation axis $\hat{\boldsymbol{n}}_{\text{map}}$ is a mapping of $\hat{\boldsymbol{n}}_0$ in a new Poincaré sphere by coordinate rotation of the Poincaré sphere of local SOPs.

According the results above, the exponential term $[-2\alpha\Delta z + \hat{\boldsymbol{n}}_{\text{map}}(2\Delta\beta\Delta z)]$ can be calculated out, and the calculation within every small segment is made from start point recursively. Therefore, taking advantage of the output Stokes quaternion of three adjacent points, the Stokes quaternions which describe the polarization properties of two neighboring segments in the fiber can be calculated out more concisely. This can be called the three point quaternion method.

4. Experiment of the Birefringence Quaternion Distribution Measurement in an Optical Fiber

The measurement system of the local birefringence quaternion distribution is shown in Fig. 3.

The output laser beam with wavelength 1555.9 nm from Distributed Feedback (DFB) laser is modulated by a $LiNbO_3$ Modulator, which is driven by the pulse pattern generator (PPG). The modulated light pulse propagates through an Erbium Doped Fiber Amplifier (EDFA), an optical filter and an optical circulator into the fiber under test, and the backward Rayleigh scattering optical pulse of fiber propagates through another group of EDFA and optical filter. Ultimately, the Stokes parameters of the filtered backward optical pulse are measured by our self-developed high-speed SOP detection system.

In our high-speed SOP detection system, the optical pulse returned from the fiber under test is averagely divided into 4 beams by a 1×4 optical fiber coupler. The optical pulse in the first path is used to detect its total power, namely Stokes parameter s_0. In the other three paths, every optical pulse propagates through a polarization controller (PC) and a polarization beam splitter (PBS), and the output orthogonal polarized lights from PBS are detected by a differential photodetector. By calibrating the PCs of the three paths, the six output optical powers $I_{0^\circ}, I_{90^\circ}, I_{45^\circ}, I_{-45^\circ}, I_{\text{rcp}}, I_{\text{lcp}}$ from the three PBS can match the corresponding polarization directions. According to the total optical power and the three output voltage values measured by the photodetectors, Stokes parameters s_0, s_1, s_2, s_3 could be calculated out accurately.

The backward Rayleigh scattering waveforms of Stokes parameters s_1, s_2, s_3 along a 1 km optical fiber under test are shown in Fig. 4.

Fig. 5 is the output Stokes vectors evolution trace on the Poincaré sphere directly converted from the backward Rayleigh scattering waveforms.

Due to the polarization rotation angle of the backward Rayleigh scattering light in a short length Δz is two times of the true polarization rotation angle along the optical fiber under test, in order to obtain the true SOP evolution process of the input signal light along the optical fiber, the waveforms data must be processed by half-value compression in every short segment Δz. Fig. 6 is the calculated true evolution trace of Stokes vectors on the Poincaré sphere for the input signal light along the optical fiber under test.

Further, the birefringence quaternions have the ability to make Stokes vector rotate, and the exponential term $\hat{\boldsymbol{n}}_0\Delta\beta\Delta z$(or $\hat{\boldsymbol{n}}_{\text{map}}\Delta\beta\Delta z$) of the exponential quaternion can be calculated out. The action steps are elaborated as below.

The physical meaning of exponential birefringence quaternion is shown in Fig. 7, where $\hat{\boldsymbol{n}}_{\text{map}}$ is the normal vector of the plane which is defined by the endpoints of the vector $\boldsymbol{S}_A(z)$, $\boldsymbol{S}_A(B)$,

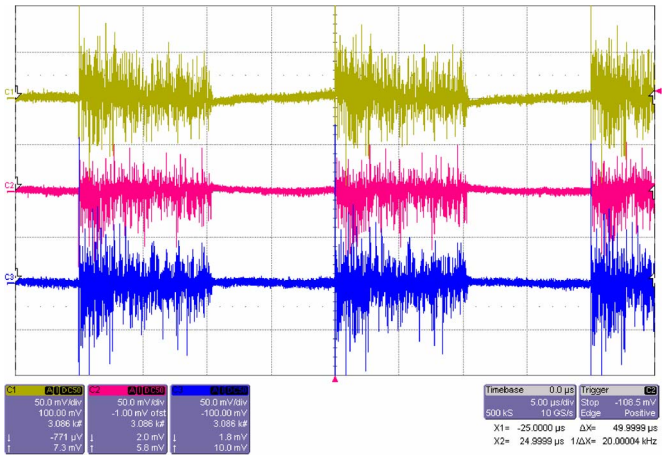

Fig. 4. Stokes parameter waveforms along a 1-km optical fiber at 1555.9 nm wavelength.

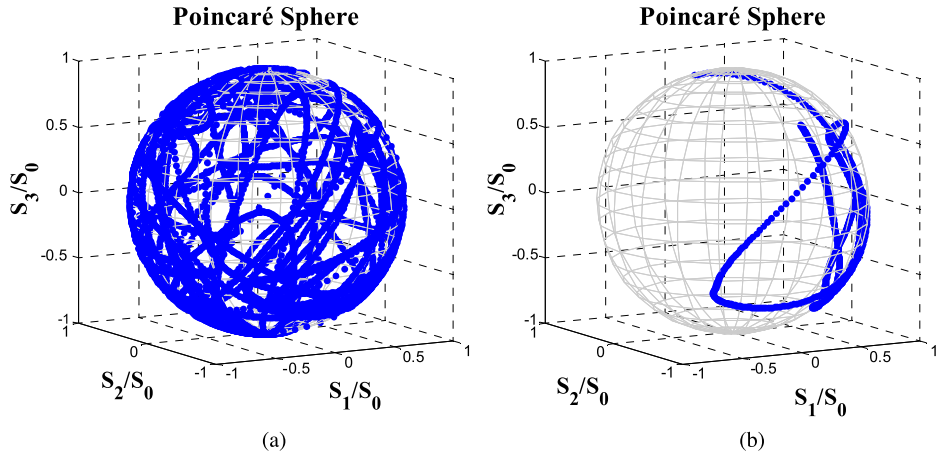

Fig. 5. Output Stokes vectors evolution trace on the Poincaré sphere. (a) 0 ∼ 1 km. (b) 0 ∼ 100 m.

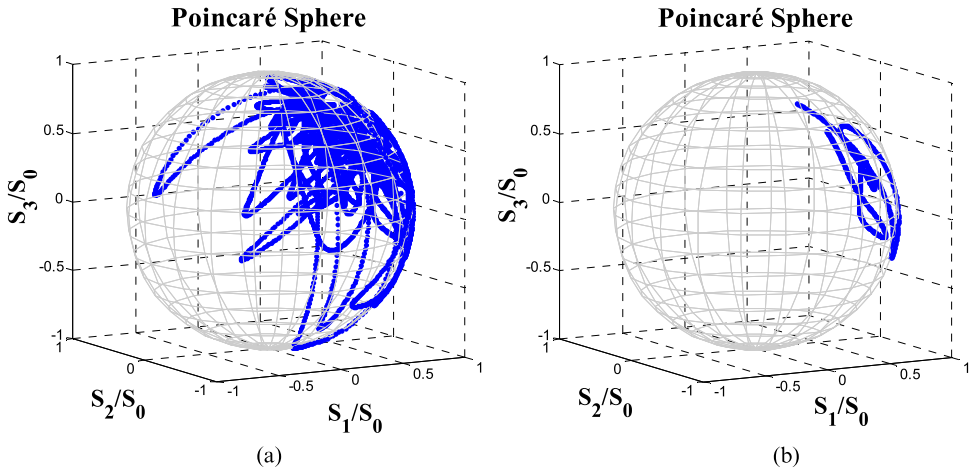

Fig. 6. True Stokes vectors evolution trace of the input signal light on the Poincaré sphere. (a) 0 ∼ 1 km. (b) 0 ∼ 100 m.

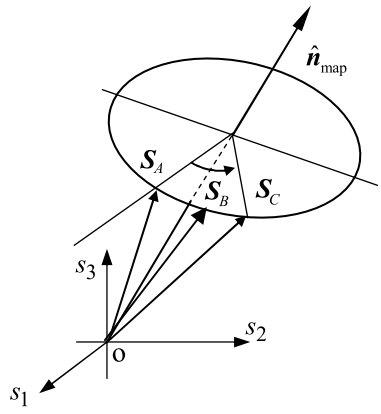

Fig. 7. Schematic of birefringence quaternion calculation $\boldsymbol{S}_A = \boldsymbol{S}_A(z)$, $\boldsymbol{S}_B = \boldsymbol{S}_A(B)$, and $\boldsymbol{S}_c = \boldsymbol{S}_A(C)$.

and $\boldsymbol{S}_A(C)$, and the rotation angle is $\Delta\beta\Delta z$, namely the magnitude of birefringence. Assuming that the coordinates of $\boldsymbol{S}_A(z)$, $\boldsymbol{S}_A(B)$, and $\boldsymbol{S}_A(C)$ are described as

$$\boldsymbol{S}_A(z) = [s_{x1}\ s_{y1}\ s_{z1}]^{\mathrm{T}}, \quad \boldsymbol{S}_A(B) = [s_{x2}\ s_{y2}\ s_{z2}]^{\mathrm{T}}, \quad \boldsymbol{S}_A(C) = [s_{x3}\ s_{y3}\ s_{z3}]^{\mathrm{T}}. \tag{39}$$

Further, we define the parameters Δ_x, Δ_y, and Δ_z as

$$\begin{cases} \Delta_x = (s_{y2} - s_{y1})(s_{z3} - s_{z1}) - (s_{y3} - s_{y1})(s_{z2} - s_{z1}) \\ \Delta_y = (s_{x2} - s_{x1})(s_{z3} - s_{z1}) - (s_{x3} - s_{x1})(s_{z2} - s_{z1}) \\ \Delta_z = (s_{x2} - s_{x1})(s_{y3} - s_{y1}) - (s_{x3} - s_{x1})(s_{y2} - s_{y1}). \end{cases} \tag{40}$$

Then, the normal vector $\hat{\boldsymbol{n}}_{\mathrm{map}}$ can be expressed as

$$\hat{\boldsymbol{n}}_{\mathrm{map}} = [\Delta_x, -\Delta_y, \Delta_z]^{\mathrm{T}}/\Delta_{\mathrm{total}} \tag{41}$$

where $\Delta_{\mathrm{total}} = (\Delta_x^2 + \Delta_y^2 + \Delta_z^2)^{1/2}$. The three endpoints of the vector $\boldsymbol{S}_A(z)$, $\boldsymbol{S}_A(B)$, and $\boldsymbol{S}_A(C)$ can define a circle, and the coordinate of the circle center is defined as $P_0(x_0, y_0, z_0)$, which can be calculated by

$$\begin{cases} x_0 = \Delta_x(\Delta_x s_{x1} - \Delta_y s_{y1} + \Delta_z s_{z1})/\Delta_{\mathrm{total}}^2 \\ y_0 = -\Delta_y(\Delta_x s_{x1} - \Delta_y s_{y1} + \Delta_z s_{z1})/\Delta_{\mathrm{total}}^2 \\ z_0 = \Delta_z(\Delta_x s_{x1} - \Delta_y s_{y1} + \Delta_z s_{z1})/\Delta_{\mathrm{total}}^2. \end{cases} \tag{42}$$

The radius of this circle is defined as ρ, and the radius of Poincaré sphere is 1, thus $\rho = [1 - (x_0^2 + y_0^2 + z_0^2)]^{1/2}$. The chord length from endpoint $\boldsymbol{S}_A$ to $\boldsymbol{S}_C$ is defined as l, which can be calculated by

$$l = \left[(s_{x3} - s_{x1})^2 + (s_{y3} - s_{y1})^2 + (s_{z3} - s_{z1})^2\right]^{1/2}. \tag{43}$$

The angular separation of these two endpoints is defined as θ (radian), which can be calculated by

$$\theta = \Delta\beta\Delta z = 2\arcsin(l/2\rho). \tag{44}$$

Therefore, if $\boldsymbol{S}_A(z)$, $\boldsymbol{S}_A(B)$, and $\boldsymbol{S}_A(C)$ are obtained, the corresponding quaternion $\exp(\hat{\boldsymbol{n}}_0\Delta\beta\Delta z)$ can be calculated by the three point quaternion method.

Utilizing this method, the calculated results shown in Fig. 6, the direction change of the birefringence quaternion along the optical fiber under test is shown in Fig. 8.

It can be seen in Fig. 8, the rotation axes of the birefringent quaternion are not equally distributed, but concentrated in two points. This result indicates that the optical fiber has some

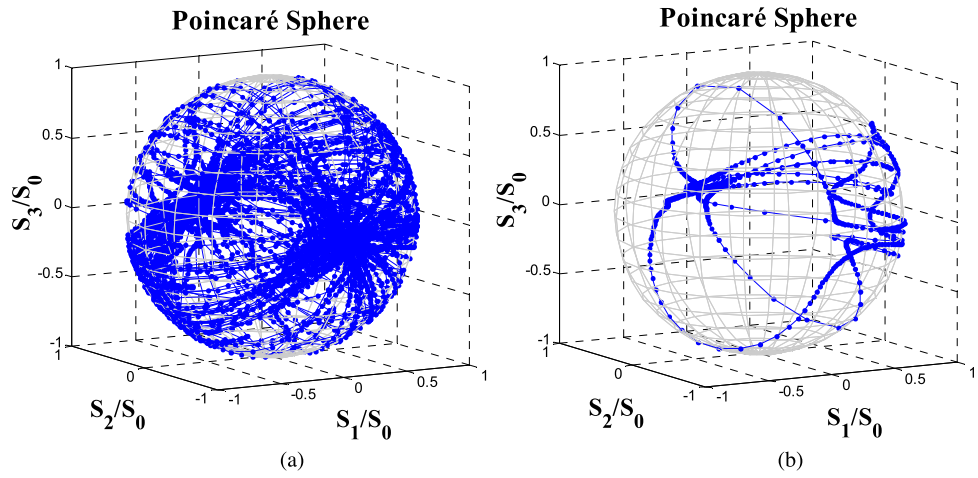

Fig. 8. Vector $\hat{\boldsymbol{n}}_0$ endpoint evolution trace of the birefringence quaternion along the optical fiber on the Poincaré sphere. (a) 0 $\sim$ 1 km. (b) 0 $\sim$ 100 m.

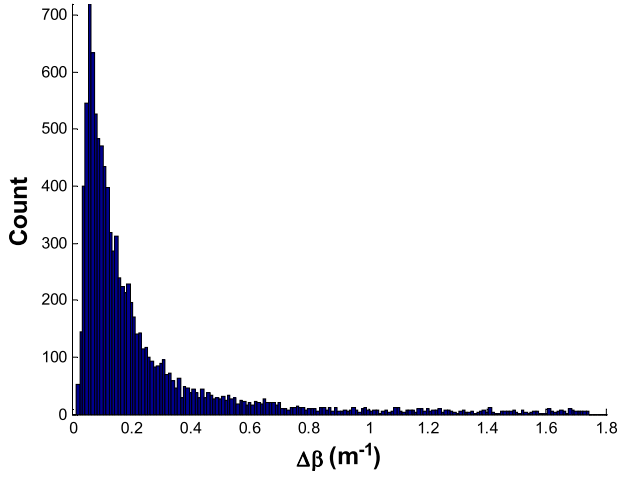

Fig. 9. Histogram for the magnitude of rotating parts in the birefringence quaternions.

inherent birefringence and has some random variation. Fig. 9 shows the histogram for the magnitude of rotating parts in the calculated birefringence quaternions, where the average value of $\Delta\beta$ is 0.2361 m^{-1}, and the corresponding average beat length is 26.6 m.

5. Error Estimation by Quaternion Interpolation Method

In the three point quaternion method, it is assumed that the local birefringence quaternions at the three points are the same, but if a relatively large change of birefringence exists, there will be an error. To estimate this error, we proposed an error estimation method by quaternion interpolation.

Assuming that the distances among the three points A, B, and C are Δz in Fig. 10, then the exponential term of the birefringence quaternion at these three points can be described as $\hat{\boldsymbol{n}}_0\Delta\beta_0$ by the three point quaternion method. In order to estimate the error, we inserted the midpoint B' between A and B, and the midpoint C' between B and C. Then the two different exponential term of the birefringence quaternions at points (A, B', B) and points (B, C', C) can be described as $\hat{\boldsymbol{n}}_1\Delta\beta_1$ and $\hat{\boldsymbol{n}}_2\Delta\beta_2$. Theoretically, the distances $\Delta z/2$ among these points are smaller, therefore a exponential term of a equivalent birefringence quaternion $\hat{\boldsymbol{n}}_{eq}\Delta\beta_{eq}$

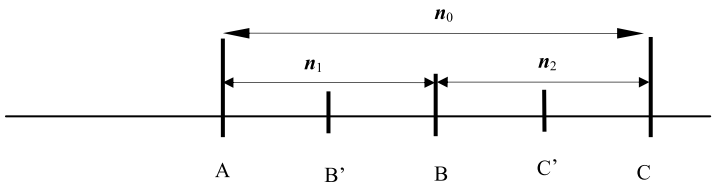

Fig. 10. Schematic of error estimation method by quaternion interpolation.

calculated by $\hat{\boldsymbol{n}}_1\Delta\beta_1$ and $\hat{\boldsymbol{n}}_2\Delta\beta_2$ should be more accurate than $\hat{\boldsymbol{n}}_0\Delta\beta_0$. The difference $\delta = |(\hat{\boldsymbol{n}}_{\text{eq}}\Delta\beta_{\text{eq}} - \hat{\boldsymbol{n}}_0\Delta\beta_0)|/\Delta\beta_0$ can be used to express the relative error of $\hat{\boldsymbol{n}}_0\Delta\beta_0$.

In addition, we need to deduce the quaternion for describing the cascaded polarization optical components. When multiple optical components are cascaded, if the polarization characteristic of each component can be described by respective Mueller quaternion, the total Mueller quaternion can be described by the product of all the components Mueller quaternions. However, since each quaternion of all components is exponential type, therefore it must be considered that when two quaternions are exponentially multiplied, whether the exponential terms can be added. For this purpose, we introduce the analogous operation of Baker–Campbell–Hausdorff formula.

The question is that if $\mathscr{M}_1 = \exp(\mathscr{A}_1)$, $\mathscr{M}_2 = \exp(\mathscr{A}_2)$, whether the result of $\mathscr{M}_1 \circ \mathscr{M}_2 = \exp(\mathscr{A}_1) \circ \exp(\mathscr{A}_2)$ is equal to $\exp(\mathscr{A}_1 + \mathscr{A}_2)$. Therefore, we introduce the quaternion commutative operation described by

$$[\mathscr{A}, \mathscr{B}] = \mathscr{A} \circ \mathscr{B} - \mathscr{B} \circ \mathscr{A}. \tag{45}$$

Equation (46), shown below, can be proved easily

$$[\mathscr{A}, \mathscr{B}] = 2\boldsymbol{A} \times \boldsymbol{B}. \tag{46}$$

According to the equivalence theorem for matrix operation and quaternion operation discussed above, (47), shown below, can be proved utilizing matrix multiplication (Campbell–Baker–Hausdorff formula) [22]

$$\exp(\mathscr{A})\exp(\mathscr{B}) = \exp\left(\mathscr{A} + \mathscr{B} + \frac{[\mathscr{A}, \mathscr{B}]}{2} + \frac{[[\mathscr{A}, [\mathscr{A}, \mathscr{B}]] + [[\mathscr{B}, \mathscr{A}], \mathscr{B}]]}{12} + \cdots\right). \tag{47}$$

When the two quaternions have only the vector parts, a special case described by and will exist as

$$\exp(\boldsymbol{A})\exp(\boldsymbol{B}) = \exp\left(\boldsymbol{A} + \boldsymbol{B} + \boldsymbol{A} \times \boldsymbol{B} + \frac{1}{3}[\boldsymbol{A} \times [\boldsymbol{A} \times \boldsymbol{B}] + [\boldsymbol{A} \times \boldsymbol{B}] \times \boldsymbol{B}] + \cdots\right). \tag{48}$$

Obviously, when $\boldsymbol{A}$ and $\boldsymbol{B}$ have the same direction, the exponential terms can be added. This is also the basis for the deducing (22) from (21).

However, when $\boldsymbol{A} \times \boldsymbol{B} \neq 0$, the exponential terms cannot be added, but when $\boldsymbol{A} \times \boldsymbol{B} = [\boldsymbol{A}, \boldsymbol{B}]/2$ is a small value (usually occurring in optical fibers), it means that the two vectors are approximately parallel (also known as the paraxial approximation), then by ignoring the higher order terms, the approximate result is written as

$$\exp(\boldsymbol{A})\exp(\boldsymbol{B}) \approx \exp(\boldsymbol{A} + \boldsymbol{B} + \boldsymbol{A} \times \boldsymbol{B}). \tag{49}$$

This equation is similar to the Baker–Campbell–Hausdorff formula which is used to calculate the multiplication of the exponential matrices with the same base. We might call it the quaternion Baker–Campbell–Hausdorff formula under paraxial approximation.

Applying (49) to the model in Fig. 10, assuming that the Stokes quaternion at position A is expressed as $\mathscr{S}(A)$, and the Stokes quaternion $\mathscr{S}(B)$ at position B evolved from point A can be written as

$$\mathscr{S}(B) = e^{\hat{\boldsymbol{n}}_1\Delta\beta_1\Delta z/4} \circ \mathscr{S}(A) \circ e^{-\hat{\boldsymbol{n}}_1\Delta\beta_1\Delta z/4} = e^{\hat{\boldsymbol{n}}_1\Delta\beta_1\Delta z/4} \circ \mathscr{S}(A) \circ (c, c) \tag{50}$$

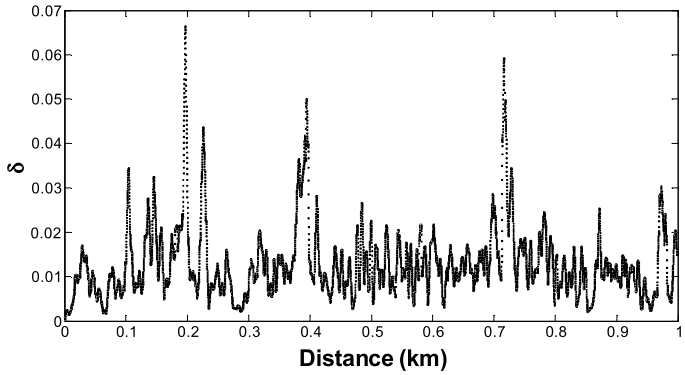

Fig. 11. Relative error distribution along the optical fiber under test.

where (c, c) is the conjugate of the quaternion before. The Stokes quaternion $\mathscr{S}_A(B)$ at position A reflected from point B can be written as

$$\mathscr{S}_A(B) = e^{[\hat{\boldsymbol{n}}_1 \Delta\beta_1 \Delta z/2]} \circ \mathscr{S}(A) \circ (c, c). \tag{51}$$

In addition, the Stokes quaternion $\mathscr{S}(C)$ at point C evolved from point B can be written as

$$\mathscr{S}(C) = e^{\hat{\boldsymbol{n}}_2 \Delta\beta_2 \Delta z/4} \circ \mathscr{S}(B) \circ (c, c). \tag{52}$$

The Stokes quaternion $\mathscr{S}'_A(C)$ at point A reflected from point C through point B can be written as

$$\mathscr{S}'_A(C) = e^{\hat{\boldsymbol{n}}_1 \Delta\beta_1 \Delta z/4} \circ e^{\hat{\boldsymbol{n}}_2 \Delta\beta_2 \Delta z/4} \circ e^{\hat{\boldsymbol{n}}_2 \Delta\beta_2 \Delta z/4} \circ e^{\hat{\boldsymbol{n}}_1 \Delta\beta_1 \Delta z/4} \circ \mathscr{S}(A) \circ (c, c). \tag{53}$$

Utilizing the quaternion Baker–Campbell–Hausdorff formula (44), $\mathscr{S}'_A(C)$ can be obtained through complex calculations. Ultimately, $\mathscr{S}'_A(C)$ can be expressed as

$$\mathscr{S}'_A(C) = \exp[\hat{\boldsymbol{n}}_2(\Delta\beta_2 \Delta z/2) + \hat{\boldsymbol{n}}_1(\Delta\beta_1 \Delta z/2) + (\hat{\boldsymbol{n}}_2 \times \hat{\boldsymbol{n}}_1)(\Delta\beta_1 \Delta z)(\Delta\beta_2 \Delta z)/4] \circ \mathscr{S}(A) \circ (c.c). \tag{54}$$

On the other hand, the Stokes quaternion $\mathscr{S}_A(C)$ directly calculated from the point A, B, and C is expressed as

$$\mathscr{S}_A(C) = e^{(\hat{\boldsymbol{n}}_0 \Delta\beta_0 \Delta z)} \circ \mathscr{S}(A) \circ (c.c). \tag{55}$$

Therefore, the relative error of the local birefringence quaternion described as δ can be calculated by

$$\begin{aligned} \delta &= \left|(\hat{\boldsymbol{n}}_{\text{eq}} \Delta\beta_{\text{eq}} - \hat{\boldsymbol{n}}_0 \Delta\beta_0)\right| / \Delta\beta_0 \\ &= |\hat{\boldsymbol{n}}_2(\Delta\beta_2/2) + \hat{\boldsymbol{n}}_1(\Delta\beta_1/2) + (\hat{\boldsymbol{n}}_2 \times \hat{\boldsymbol{n}}_1)(\Delta\beta_1)(\Delta\beta_2)\Delta z/4 - \hat{\boldsymbol{n}}_0 \Delta\beta_0| / \Delta\beta_0. \end{aligned} \tag{56}$$

As can be seen from the (56), the smaller $|\Delta z|$ is, the smaller the relative error will be.

Using (56) and the data shown in Fig. 6, the relative error distribution along the optical fiber under test can be calculated out, which is shown in Fig. 11. As can be seen from the figure, the maximal error is less than 7%, and the average error is 1.3%.

6. Conclusion

We proposed a method to convert Jones vector into quaternion, and proved that Stokes quaternion is double product of Jones quaternion and its Hermitian transpose. Then, the quaternion

descriptions for the polarization properties of optical components with polarization dependent phase shift (birefringence) and polarization dependent loss (PDL) were discussed. Moreover, the multiplication of the exponential quaternions which describe the cascaded optical components can be expressed as Baker–Campbell–Hausdorff formula under paraxial approximation condition.

The quaternion theories above for polarization optics were applied in the measurement of local birefringence distribution based on our self-developed high-speed SOP detected P-OTDR system in this paper. We proved that the rotation axis of the output three adjacent points Stokes quaternions is a mapping from the rotation axis of the three adjacent reflection points Stokes quaternions in the optical fiber under test by coordinate rotation of the Poincaré sphere, and the rotation angle among the output three adjacent points is the doubleness of the rotation angle among the three adjacent reflection points in the optical fiber. Then we proposed the three point quaternion method and completed the measurement of the local birefringence distribution by these Stokes quaternions. Ultimately, we proposed a relative error estimation method based on the parallel approximate quaternion Baker–Campbell–Hausdorff formula of exponential quaternions. The result showed the average birefringence quaternion is $0.263/m^{-1}$ in the optical fiber under test (corresponding average beat length is 26 m), and the average relative measurement error is less than 1.3%.

References

[1] V. Ramaswamy, W. G. French, and R. D. Standley, "Polarization characteristics of noncircular core single-mode fibers," *Appl. Opt.*, vol. 17, no. 18, pp. 3014–3017, Sep. 1978.

[2] K. Iwatsuki, K. Hotate, and M. Higashiguchi, "Eigenstate of polarization in a fiber ring resonator and its effect in an optical passive ring-resonator gyro," *Appl. Opt.*, vol. 25, no. 15, pp. 2606–2612, Aug. 1986.

[3] N. Peng *et al.,* "Fiber optic current sensor based on special spun highly birefringent fiber," *IEEE Photon. Technol. Lett.*, vol. 25, no. 17, pp. 1668–1671, Sep. 2013.

[4] S. C. Rashleigh and R. Ulrich, "Polarization mode dispersion in single mode fibers," *Opt. Lett.*, vol. 3, no. 2, pp. 60–62, Aug. 1978.

[5] C. D. Poole, J. H. Winters, and J. A. Nagel, "Dynamical equation for polarization dispersion," *Opt. Lett.*, vol. 18, no. 6, pp. 372–374, Mar. 1991.

[6] R. Ulrich, S. Rashleigh, and W. Eickhoff, "Bending-induced birefringence in single-mode fibers," *Opt. Lett.*, vol. 5, no. 6, pp. 273–275, Jun. 1980.

[7] U. L. Block *et al.,* "Bending-induced birefringence of optical fiber cladding modes," *J. Lightw. Technol.*, vol. 24, no. 6, pp. 2336–2339, Jun. 2006.

[8] A. J. Rogers, "Polarization-optical time domain reflectometry: A technique for the measurement of field distributions," *Appl. Opt.*, vol. 20, no. 6, pp. 1060–1074, Mar. 1981.

[9] J. N. Ross, "Birefringence measurement in optical fibers by polarization optical time-domain reflectometry," *Appl. Opt.*, vol. 21, no. 19, pp. 3489–3495, Oct. 1982.

[10] S. Y. Huang and Z. Q. Lin, "Measuring the birefringence of single-mode fibers with short beat length or nonuniformity: A new method," *Appl. Opt.*, vol. 24, no. 15, pp. 2355–2361, Aug. 1985.

[11] T. Chartier, A. Hideur, C. Özkul, F. Sanchez, and G. M. Stéphan, "Measurement of the elliptical birefringence of single-mode optical fibers," *Appl. Opt.*, vol. 40, no. 30, pp. 5343–5353, Oct. 2001.

[12] J. G. Ellison and A. S. Siddiqui, "Using polarimetric optical time domain reflectometry to extract spun fiber parameters," *Proc. Inst. Elect. Eng.—Optoelectron.*, vol. 148, no. 4, pp. 176–182, Aug. 2001.

[13] M. Wuilpart, P. Mégret, M. Blondel, A. J. Rogers, and Y. Defosse, "Measurement of the spatial distribution of birefringence in optical fibers," *IEEE Photon. Technol. Lett.*, vol. 13, no. 8, pp. 836–838, Aug. 2001.

[14] S. Yang, C. Wu, and Z. Li, "Demonstration of piezoelectric polarization controller assisted P-OTDR," presented at the Opt. Fiber Commun. Conf., San Diego, CA, USA, 2009, Paper JWA79.

[15] W. R. Hamilton, "On a new species of imaginary quantities connected with a theory of Quaternions," in *Proc. Meet. Royal Irish Acad.*, Nov. 1848, pp. 1–16. [Online]. Available: http://www.maths.tcd.ie/pub/HistMath/People/Hamilton/Quaternions.html

[16] M. Karlsson and M. Petersson, "Quaternion approach to PMD and PDL phenomena in optical fiber systems," *J. Lightw. Technol.*, vol. 22, no. 4, pp. 1137–1146, Apr. 2004.

[17] D. Guangtao, "Quaternion method in polarization optics," *Acta Opt. Sin.*, vol. 33, no. 7, 2013, Art. ID. 0726001, (in Chinese).

[18] L. Liu, C. Wu, and Z. Li, "Investigation of polarization state generation with ergodicity of polarization states based on the quaternion approach," *Acta Opt. Sin.*, vol. 34, no. 3, 2014, Art. ID. 0306002, (in Chinese).

[19] H. Henry and R. C. Jones, "A new calculus for the treatment of optical systems," *J. Opt. Soc. Amer.*, vol. 31, no. 7, pp. 488–493, Jul. 1941.

[20] W. S. Bickel and W. M. Bailey, Stokes vectors Mueller matrices and polarized light scattering," *Am. J. Phys*, vol. 53, no. 5, pp. 468–478, May 1985.

[21] H. Mueller, "The foundation of optics (Abstract)," *J. Opt. Soc. Amer.*, vol. 38, pp. 661–672, 1948.

[22] Wikipedia, *Baker–Campbell–Hausdorff Formula*, May 2015. [Online]. Available: http://en.wikipedia.org/wiki/Baker%E2%80%93Campbell%E2%80%93Hausdorff_formula